Channels 5:4, 320-324; July/August 2011; © 2011 Landes Bioscience

Calmodulin overexpression does not alter $Ca_v1.2$ function or oligomerization state

Felix Findeisen,[1] Alexandra Tolia,[1] Ryan Arant,[7] Eun Young Kim,[1] Ehud Y. Isacoff[5-7] and Daniel L. Minor, Jr.[1-4,*]

[1]Cardiovascular Research Institute; [2]Departments of Biochemistry and Biophysics; and Cellular and Molecular Pharmacology; [3]California Institute for Quantitative Biomedical Research; University of California, San Francisco; San Francisco, CA USA [4]Physical Biosciences and [5]Materials Science Divisions; Lawrence Berkeley National Laboratory; [6]Helen Wills Neuroscience Institute; [7]Department of Molecular and Cell Biology; University of California, Berkeley; Berkeley, CA USA

Interactions between calmodulin (CaM) and voltage-gated calcium channels (Ca_vs) are crucial for Ca_v activity-dependent feedback modulation. We recently reported an X-ray structure that shows two Ca^{2+}/CaM molecules bound to the $Ca_v1.2$ C-terminal tail, one at the PreIQ region and one at the IQ domain. Surprisingly, the asymmetric unit of the crystal showed a dimer in which Ca^{2+}/CaM bridged two PreIQ helixes to form a 4:2 Ca^{2+}/CaM:Ca_v C-terminal tail assembly. Contrary to previous proposals based on a similar crystallographic dimer, extensive biochemical analysis together with subunit counting experiments of full-length channels in live cell membranes failed to find evidence for multimers that would be compatible with the 4:2 crossbridged complex. Here, we examine this possibility further. We find that CaM overexpression has no functional effect on $Ca_v1.2$ inactivation or on the stoichiometry of full-length $Ca_v1.2$. These data provide further support for the monomeric $Ca_v1.2$ stoichiometry. Analysis of the electrostatic surfaces of the 2:1 Ca^{2+}/CaM:Ca_v C-terminal tail assembly reveals notable patches of electronegativity. These could influence various forms of channel modulation by interacting with positively charged elements from other intracellular channel domains.

Key words: voltage-gated calcium channel, $Ca_v1.2$, calmodulin, calcium-dependent inactivation (CDI), stoichiometry

Submitted: 05/28/11

Revised: 06/03/11

Accepted: 06/05/11

DOI:10.4161/chan.5.4.16821

*Correspondence to: Daniel L. Minor; Email: daniel.minor@ucsf.edu

Addendum to: Kim EY, Rumpf CH, Van Petegem F, Arant RJ, Findeisen F, Cooley ES, et al. Multiple C-terminal tail Ca^{2+}/CaMs regulate $Ca_v1.2$ function but do not mediate channel dimerization. EMBO J 2010; 29:3924–38; PMID: 20953164; DOI: 10.1038/emboj.2010.260.

Introduction

High-voltage activated voltage-gated calcium channels (Ca_v1s and Ca_v2s) couple membrane depolarization dependent calcium entry to many physiological processes.[1,2] These channels are multisubunit complexes that include a $Ca_v\alpha_1$ pore-forming subunit, the auxiliary proteins $Ca_v\beta$, $Ca_v\alpha_2\delta$ and calmodulin (CaM).[1,3,4] Calcium-calmodulin (Ca^{2+}/CaM) has a central role in two distinct Ca_v feedback mechanisms, calcium-dependent inactivation (CDI) and calcium-dependent facilitation (CDF),[5] that involve direct interactions with the $Ca_v\alpha_1$ C-terminal cytoplasmic tail IQ domain.[6-12] Understanding the molecular basis for CaM-Ca_v interactions and how these interactions affect channel function remains an important challenge that requires structural definition and biochemical analysis of key regulatory CaM binding sites.

Results and Discussion

We recently reported the structure of a complex of Ca^{2+}/CaM and a segment of the $Ca_v1.2$ C-terminal tail that encompasses the PreIQ and IQ domains (residues 1,561–1,637).[8] Ca^{2+}/CaM has two lobes, N-lobe and C-lobe, which can each engage target-binding partners. Consequently, a number of diverse Ca^{2+}/CaM-target binding modes have been reported.[13,14] The Ca^{2+}/CaM:$Ca_v1.2$ C-terminal tail complex defines two Ca^{2+}/CaM binding sites that are occupied by two separate Ca^{2+}/CaMs. Each interacts with the channel in distinct ways (**Fig. 1A**). One Ca^{2+}/CaM engages the IQ domain using both lobes

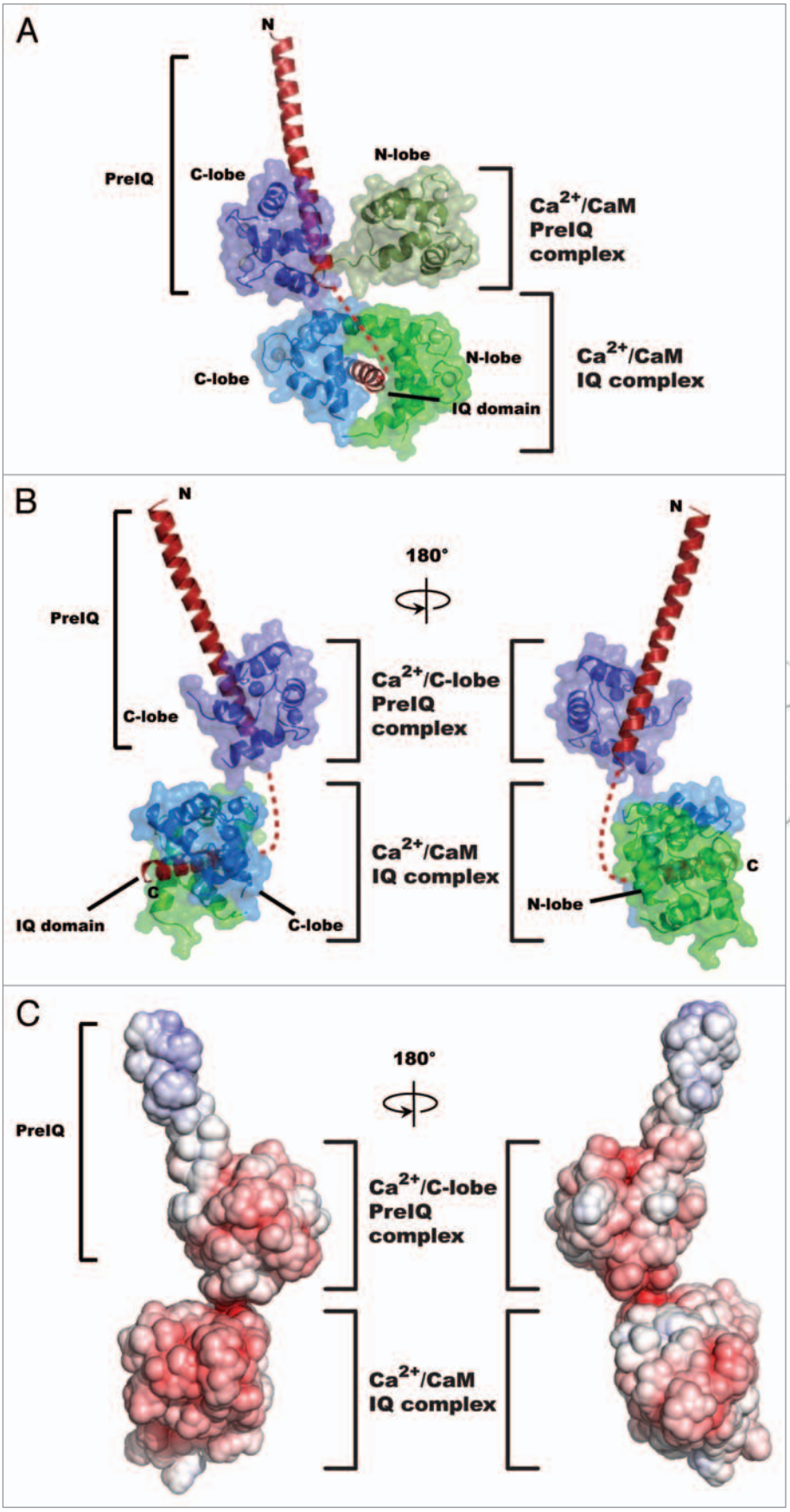

Figure 1. Structure of the 2:1 Ca^{2+}/CaM:$Ca_v1.2$ C-terminal tail complex. (A) Cartoon diagram of the Ca^{2+}/CaM:$Ca_v1.2$ C-terminal tail complex. The $Ca_v1.2$ C-terminal tail is shown in red. Ca^{2+}/CaM molecules bound to the PreIQ and domains are indicated. In both cases Ca^{2+}/CaM is shown using a surface representation and the Ca^{2+}/N-lobes and Ca^{2+}/C-lobes of the PreIQ bound and IQ bound Ca^{2+}/CaMs are colored forest and dark blue, and green and marine, respectively. (B) Cartoon diagram as in '(A)' but lacking the Ca^{2+}/N-lobe from the PreIQ Ca^{2+}/CaM. Colors as in (A). (C) Surface charge representation of the 2:1 Ca^{2+}/CaM:Ca_v C-terminal tail shown in the same orientation as '(B)'. Colors indicate a scale from -10 kT/e (red) to + 10kT/e (blue).

in a manner identical to prior structures of Ca^{2+}/CaM-$Ca_v1.2$ IQ domain complex.[12,15] In contrast, the second Ca^{2+}/CaM binds the C-terminal segment of the long PreIQ helix using only Ca^{2+}/C-lobe. Notably, the association of CaM with the PreIQ-IQ segment creates a number of electronegative patches (**Fig. 1B and C**). These patches raise the possibility that positively charged residues elsewhere in the channel form key interactions with this segment.

Biochemical studies revealed that the two Ca^{2+}/CaMs have very different properties. The Ca^{2+}/CaM molecule bound to the PreIQ segment is labile and could be removed by passage over a phenyl-sepharose column in conditions of high-calcium (2 mM). In contrast, the Ca^{2+}/CaM on the IQ domain remained bound. Further, functional studies indicated that the PreIQ site has a role in calcium-dependent facilitation (CDF).[8] Extensive biophysical characterization showed that the complex maintains a 2:1 Ca^{2+}/CaM:C-terminal tail stoichiometry even at protein concentrations that match those found in the most densely packed native Ca_v environment (≥100 μM). Together, these studies demonstrate that the $Ca_v1.2$ C-terminal tail can bind two Ca^{2+}/CaMs simultaneously and suggest that the Ca^{2+}/CaM occupying the PreIQ binding site is poised to make interactions with other elements of the channel by virtue of the free Ca^{2+}/N-lobe.

A curious feature of the asymmetric unit of the Ca^{2+}/CaM:PreIQ-IQ

complex was that it contained two Ca^{2+}/CaM:PreIQ-IQ complexes that interacted through a portion of the PreIQ domain and was bridged by the PreIQ-Ca^{2+}/CaMs. A similar X-ray structure led to the proposal that $Ca_v1.2$ channels dimerize via this sort of interaction and that this interaction is functionally relevant.[16] It is not straightforward to discern the relevance of protein-protein interactions from crystal lattice contacts alone as such interactions are a necessary requirement for forming a crystal lattice.[17,18] Further, there are numerous examples in which crystallographic dimers do not represent biologically relevant interactions.[19]

Our biophysical data on the isolated $Ca_v1.2$ channel tail complex clearly indicated a 2:1 stoichiometry. Although it has not been generally thought that Ca_v channels function as dimers, electron microscopy studies of full-length $Ca_v1.2$ [20,21] and the observation of infrequent multiple concerted $Ca_v1.2$ openings[22] have suggested that under some conditions the full-length channel may form higher order assemblies. To address the question of $Ca_v1.2$ oligomerization state in live cell membranes directly, we used total internal reflection fluorescence microscopy (TIRFM) [23] and $Ca_v1.2$ bearing a C-terminal green fluorescent protein (GFP) tag for single-molecule subunit counting. Our studies showed unambiguously that the $Ca_v1.2$ channels are monomeric.[8] Importantly, the Navedo et al. study showed that deletion of a large section of the C-terminal tail (D1670X), which removes all of the C-terminal tail after the IQ domain, eliminates all measurable multichannel coupling. Thus, unlike what has been proposed by Fallon et al. the $Ca_v1.2$ 4:2 complex observed in the crystal structure is non-physiological and is not relevant for channel function. Further, whatever coupling mechanism underlies the observations of Navedo et al. it does not involve the PreIQ-IQ domain.

A key assumption of both our functional and subunit counting experiments is that the Xenopus oocytes that are used to overexpress $Ca_v1.2$ have sufficient endogenous CaM to make functional channels. Previous studies have shown that multiple alanine mutations on the channel that weaken CaM affinity for the IQ domain and reduce CDI can be overcome, at least in part, by CaM co-expression.[24,25] Because the PreIQ-bound CaM is responsible for crossbridging interactions in the asymmetric unit and is labile, we tested whether CaM overexpression would affect $Ca_v1.2$ function or oligomerization state. Injection of Xenopus oocytes with fixed amounts of $Ca_v1.2$ mRNA and either a 10-fold or 60-fold excess of CaM mRNA gave $Ca_v1.2$ channels in which both CDI and a second form of inactivation, voltage-dependent inactivation (VDI), were indistinguishable from $Ca_v1.2$ relying on endogenous CaM (**Fig. 2A and Table 1**).

To examine whether the overexpressed CaM associated with $Ca_v1.2$, we co-injected mRNA for Flag-tagged $Ca_v1.2$ and mCherry-labeled CaM at a ratio of 1:10. This combination has identical functional properties to the untagged components (**Fig. 2B and Table 1**). Both components are clearly overexpressed (**Fig. 2C**). Immunoprecipitation using anti-Flag M2 agarose to capture the $Ca_v1.2$ subunit did not detect any interaction between $Ca_v1.2$ and CaM in the absence of Ca^{2+} (**Fig. 2C**). Importantly, similar to prior reports with untagged subunits,[26] in the presence 500 μM Ca^{2+} the CaM-mCherry-$Ca_v1.2$ interaction was readily observed and directly demonstrated that overexpressed CaM binds the channel (**Fig. 2C**). These data, together with the absence of functional effects of CaM overexpression, strongly suggest that the endogenous levels of CaM present in Xenopus oocytes are sufficient to account for all $Ca_v1.2$ functional effects.

We also examined by single molecule subunit counting whether excess CaM expression influenced $Ca_v1.2$ oligomerization (**Fig. 2D–G**). TIRF images indicated that CaM-mCherry was present at the membrane. Examination of spots in which both $Ca_v1.2$-GFP and CaM-mCherry were present showed that the vast majority (95%) of $Ca_v1.2$-GFP fluorescent spots bleached in a single step (**Fig. 2F and G**). These data provide strong indication that the channels remain monomers even when excess CaM is present at the membrane and further support our interpretation that the structure of CaM bridging two PreIQ helices is not relevant for full-length channels.

Our studies demonstrate that the $Ca_v1.2$ PreIQ-IQ segment is capable of binding multiple Ca^{2+}/CaMs simultaneously and that the PreIQ site is involved in channel function.[8] The organization of multiple Ca^{2+}/CaMs along a largely helical segment is reminiscent of how CaM and CaM-like proteins are organized on myosin[27] and raises the intriguing possibility that there are previously unrecognized connections between these systems. How the Ca^{2+}/CaM:$Ca_v1.2$ C-terminal tail complex interacts with other channel elements in both the calcium-bound and calcium-free states remains a major open question. The presence of large patches of electronegative surface on the Ca^{2+}/CaM:$Ca_v1.2$ C-terminal tail complex raises the possibility that there may be positively charged residues elsewhere in the channel that form key interactions with this segment. Defining such interactions and their state-dependence remains an important goal for the field.

Methods

Two-electrode voltage clamp recordings. *Homo sapiens* CaM (GenBank NM_006888) was subcloned into pGEMHE-mCherry plasmid[28] using SacII/HindIII restriction sites. All other DNA constructs were the same as in reference 8. Generation of mRNA and electrophysiological protocols were as described previously in references 8 and 12, except where noted. In brief, Xenopus oocytes were injected with 50 nl RNA mixture of $Ca_v1.2$ (or $Ca_v1.2$-mEGFP), $Ca_v\beta_{2a}$, $Ca_v\alpha_2\delta$-1 and CaM (or CaM-mCherry) at a molar ratio of 1:1:1:10 unless indicated otherwise and recorded 2–4 days after injection. All data were produced from more than one oocyte batch and analyzed with Clampfit 9.2 (Axon Instruments).

Western blot detection of whole-cell lyates and immunoprecipitation of flag-tagged $Ca_v1.2$ from Xenopus oocytes. In each case, nineteen oocytes were injected with $Ca_v1.2$-3xFlag, $Ca_v\beta_{2a}$, $Ca_v\alpha_2\delta$ and CaM-mCherry at a molar ratio of 1:1:1:10 or water. After two days, oocytes were collected and homogenized in immunoprecipitation (IP) buffer 150 mM NaCl,

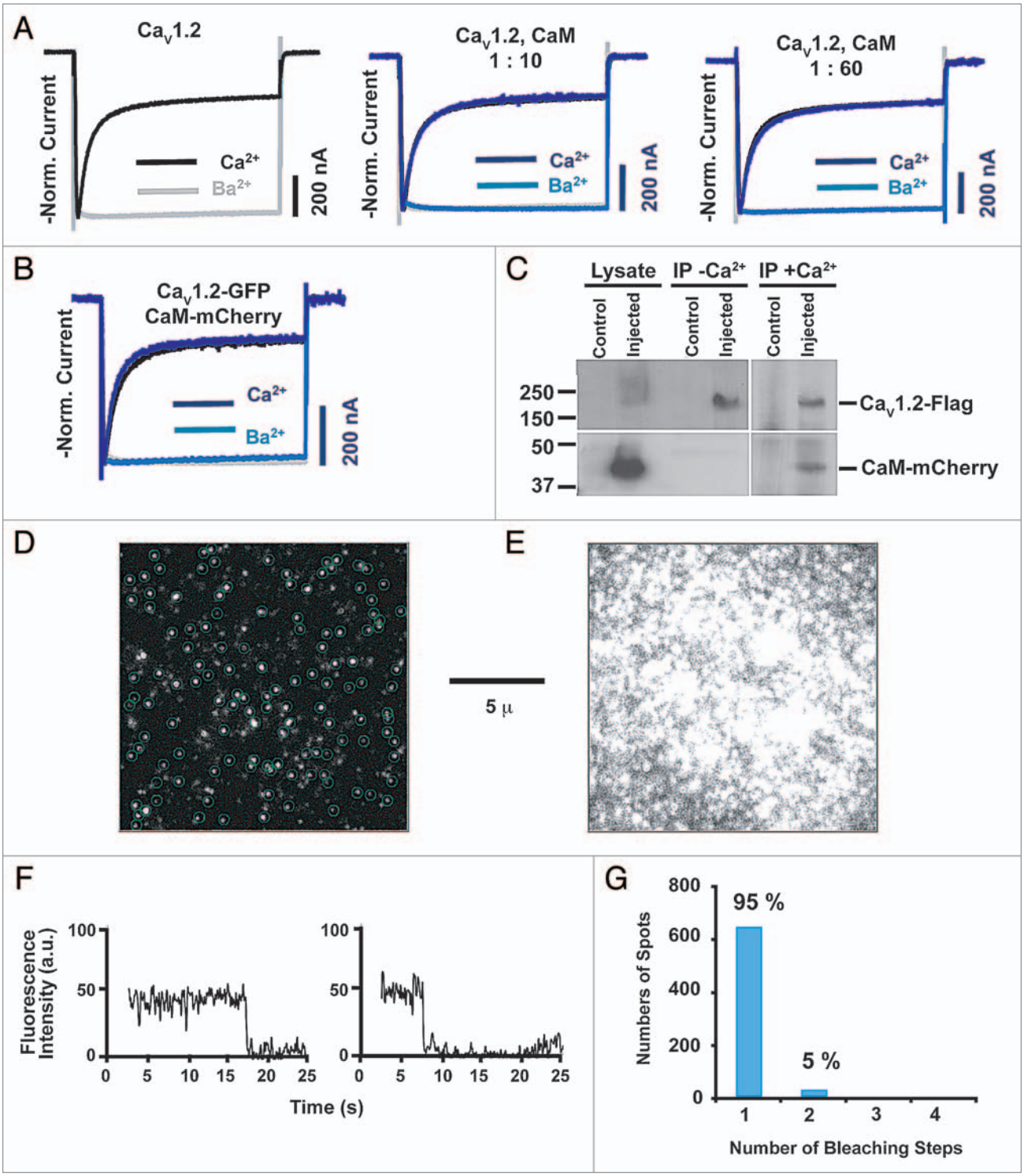

Figure 2. Effect of CaM overexpression on $Ca_v1.2$ function and stoichiometry. (A) Comparison of $Ca_v1.2$ CDI and VDI as a function of CaM overexpression. Normalized Ca^{2+} and Ba^{2+} currents for channels relying on endogenous CaM (black and gray, respectively) or with excess CaM mRNA at the indicated ratios (dark blue and light blue, respectively). (B) Normalized Ca^{2+} and Ba^{2+} currents recorded from $Ca_v1.2$-GFP co-expressed with CaM-mCherry at a mRNA ratio of 1:10 (dark blue and light blue, respectively) are compared to wild type (black and gray, respectively). Experimental details are the same as in reference 8. (C) Western blot detection of whole-cell lyates and immunoprecipitation of Flag-tagged $Ca_v1.2$ from Xenopus oocytes. Detection was with an antibody against Flag or mCherry as indicated. (D) Subunit counting of $Ca_v1.2$ in live cell membranes. A representative TIRF image showing the $Ca_v1.2$-GFP fluorescent spots at the cell surface of *X. laevis* oocytes. Bright spots are $Ca_v1.2$-GFP single-molecules when the shutter is first opened at the beginning of the bleaching experiment. Blue circles mark the selected molecules for subunit counting. (E) TIRF image showing CaM-mCherry spots in the cell surface of *X. laevis* oocytes. (F) Time courses of photobleaching from single GFP fluorescent spots. Two examples are shown. (G) Distribution of fluorescent spots that bleach in one or more steps. Percentile of each bleaching step is indicated.

Table 1. $Ca_v1.2$ inactivation parameters

	t_{i300} (%)	A_1 (%)	τ_1 (ms^{-1})	A_2 (%)	τ_2 (ms^{-1})	N
$Ca_v1.2$	69.0 ± 2.2	55.8 ± 3.2	25.0 ± 3.7	16.4 ± 1.9	138 ± 21	12
$Ca_v1.2$, CaM 1:10	67.7 ± 3.5	53.9 ± 7.3	26.7 ± 4.2	17.5 ± 5.9	136 ± 32	8
$Ca_v1.2$, CaM 1:60	69.0 ± 2.4	57.2 ± 1.7	25.0 ± 4.8	15.9 ± 3.3	142 ± 37	6
$Ca_v1.2$-GFP, CaM-Cherry 1:10	71.4 ± 7.3	55.2 ± 6.5	25.3 ± 5.3	20.5 ± 4.6	142 ± 29	8

All experiments correspond to the mean of at least two separate oocyte batches. '±' values are standard deviation.

0.5% CHAPS, 50 mM Hepes/NaOH pH 7.4 and Complete protease inhibitors (Roche), with or without 500 μM $CaCl_2$ (IP + Ca^{2+} or IP-Ca^{2+} respectively). Lysates were cleared by centrifugation at 13,000 rpm for 30 min and 600 μg of protein was incubated with 35 μl anti-Flag M2 agarose beads (Sigma-Aldrich) overnight at 4°C. Beads were washed four times with IP buffer and bound proteins were released by heating at 70°C for 10 min in NuPAGE sample buffer (Invitrogen). Samples were separated on a 4–12% NuPAGE Bis-Tris gel, transferred on nitrocellulose and reacted with either anti-FLAG monoclonal antibody (1:5,000, Sigma-Aldrich) or Living Colors DsRed polyclonal antibody (1:1,000, Clontech).

Subunit counting experiments. DNA constructs for $Ca_v1.2$-mEGFP and CaM-mCherry were the same as described above and in reference 8. RNA transcription and experimental details are as described in reference 8, except where noted below. Oocytes were injected with 50 nl of a 1:1 mixture of 500 ng/μl $Ca_v1.2$-EGFP and 100 ng/μl $Ca_v\beta_{2a}$ cRNA and 150 ng/μl CaM-mCherry cRNA.

References

1. Catterall WA. Structure and regulation of voltage-gated Ca^{2+} channels. Annu Rev Cell Dev Biol 2000; 16:521-55.
2. Hille B. Ion Channels of Excitable Membranes. Sunderland, MA: Sinauer Associates, Inc. 2001.
3. Findeisen F, Minor DL Jr. Progress in the structural understanding of voltage-gated calcium channel (Ca_v) function and modulation. Channels (Austin) 2010; 4:459-74.
4. Van Petegem F, Minor DL. The structural biology of voltage-gated calcium channel function and regulation. Biochem Soc Trans 2006; 34:887-93.
5. Dunlap K. Calcium channels are models of self-control. J Gen Physiol 2007; 129:379-83.
6. DeMaria CD, Soong TW, Alseikhan BA, Alvania RS, Yue DT. Calmodulin bifurcates the local Ca^{2+} signal that modulates P/Q-type Ca^{2+} channels. Nature 2001; 411:484-9.
7. Kim EY, Rumpf CH, Fujiwara Y, Cooley ES, Van Petegem F, Minor DL Jr. Structures of Ca_v2 Ca^{2+}/CaM-IQ domain complexes reveal binding modes that underlie calcium-dependent inactivation and facilitation. Structure 2008; 16:1455-67.
8. Kim EY, Rumpf CH, Van Petegem F, Arant RJ, Findeisen F, Cooley ES, et al. Multiple C-terminal tail Ca^{2+}/CaMs regulate $Ca_v1.2$ function but do not mediate channel dimerization. EMBO J 2010; 29:3924-38.
9. Lee A, Zhou H, Scheuer T, Catterall WA. Molecular determinants of Ca^{2+}/calmodulin-dependent regulation of $Ca_v2.1$ channels. Proc Natl Acad Sci USA 2003; 12:12.
10. Mori MX, Vander Kooi CW, Leahy DJ, Yue DT. Crystal Structure of the Ca_v2 IQ Domain in Complex with Ca^{2+}/Calmodulin: High-Resolution Mechanistic Implications for Channel Regulation by Ca^{2+}. Structure 2008; 16:607-20.
11. Peterson BZ, DeMaria CD, Adelman JP, Yue DT. Calmodulin is the Ca^{2+} sensor for Ca^{2+}-dependent inactivation of L-type calcium channels. Neuron 1999; 22:549-58.
12. Van Petegem F, Chatelain FC, Minor DL Jr. Insights into voltage-gated calcium channel regulation from the structure of the $Ca_v1.2$ IQ domain-Ca^{2+}/calmodulin complex. Nat Struct Mol Biol 2005; 12:1108-15.
13. Hoeflich KP, Ikura M. Calmodulin in action: diversity in target recognition and activation mechanisms. Cell 2002; 108:739-42.
14. Ikura M, Ames JB. Genetic polymorphism and protein conformational plasticity in the calmodulin superfamily: two ways to promote multifunctionality. Proc Natl Acad Sci USA 2006; 103:1159-64.
15. Fallon JL, Halling DB, Hamilton SL, Quiocho FA. Structure of calmodulin bound to the hydrophobic IQ domain of the cardiac $Ca_v1.2$ calcium channel. Structure 2005; 13:1881-6.
16. Fallon JL, Baker MR, Xiong L, Loy RE, Yang G, Dirksen RT, et al. Crystal structure of dimeric cardiac L-type calcium channel regulatory domains bridged by Ca^{2+}* calmodulins. Proc Natl Acad Sci USA 2009; 106:5135-40.
17. Janin J, Bahadur RP, Chakrabarti P. Protein-protein interaction and quaternary structure. Q Rev Biophys 2008; 41:133-80.
18. Ponstingl H, Henrick K, Thornton JM. Discriminating between homodimeric and monomeric proteins in the crystalline state. Proteins 2000; 41:47-57.
19. Bahadur RP, Chakrabarti P, Rodier F, Janin J. A dissection of specific and non-specific protein-protein interfaces. J Mol Biol 2004; 336:943-55.
20. Wang MC, Collins RF, Ford RC, Berrow NS, Dolphin AC, Kitmitto A. The three-dimensional structure of the cardiac L-type voltage-gated calcium channel: comparison with the skeletal muscle form reveals a common architectural motif. J Biol Chem 2004; 279:7159-68.
21. Wang MC, Velarde G, Ford RC, Berrow NS, Dolphin AC, Kitmitto A. 3D structure of the skeletal muscle dihydropyridine receptor. J Mol Biol 2002; 323:85-98.
22. Navedo MF, Cheng EP, Yuan C, Votaw S, Molkentin JD, Scott JD, et al. Increased coupled gating of L-type Ca^{2+} channels during hypertension and Timothy syndrome. Circ Res 2010; 106:748-56.
23. Ulbrich MH, Isacoff EY. Subunit counting in membrane-bound proteins. Nat Methods 2007; 4:319-21.
24. Liang H, DeMaria CD, Erickson MG, Mori MX, Alseikhan BA, Yue DT. Unified mechanisms of Ca^{2+} regulation across the Ca^{2+} channel family. Neuron 2003; 39:951-60.
25. Erickson MG, Liang H, Mori MX, Yue DT. FRET two-hybrid mapping reveals function and location of L-type Ca^{2+} channel CaM preassociation. Neuron 2003; 39:97-107.
26. Wang HG, George MS, Kim J, Wang C, Pitt GS. Ca^{2+}/calmodulin regulates trafficking of $Ca_v1.2$ Ca^{2+} channels in cultured hippocampal neurons. J Neurosci 2007; 27:9086-93.
27. Houdusse A, Gaucher JF, Krementsova E, Mui S, Trybus KM, Cohen C. Crystal structure of apo-calmodulin bound to the first two IQ motifs of myosin V reveals essential recognition features. Proc Natl Acad Sci USA 2006; 103:19326-31.
28. Yu Y, Ulbrich MH, Li MH, Buraei Z, Chen XZ, Ong AC, et al. Structural and molecular basis of the assembly of the TRPP2/PKD1 complex. Proc Natl Acad Sci USA 2009; 106:11558-63.